Sensors & Actuators: B. Chemical 341 (2021) 130006

Contents lists available at ScienceDirect

Sensors and Actuators: B. Chemical

journal homepage: www.elsevier.com/locate/snb

Detection of protamine and heparin using a promising metal organic frameworks based fluorescent molecular device BZA-BOD@ZIF-90

Lihua Liu [a], Jianan Dai [a], Yuan Ji [a], Baoxing Shen [a,*], Xing Zhang [a,*], Robert J. Linhardt [b]

[a] School of Food Science and Pharmaceutical Engineering, Nanjing Normal University, Nanjing, Jiangsu, 210023, China
[b] Department of Chemical and Biological Engineering, Center for Biotechnology and Interdisciplinary Studies, Rensselaer Polytechnic Institute, Troy, NY, 12180, USA

ARTICLE INFO

Keywords:
BODIPY
MOFs
Protamine
Heparin
Fluorescent molecular device

ABSTRACT

Herein, we designed a BODIPY-based probe (BZA-BOD@ZIF-90) with good stability through the encapsulation of metal-organic frameworks (MOFs). BZA-BOD@ZIF-90 can selectively detect protamine based on an aggregation-induced emission (AIE) effect. In the present strategy, the designed BZA-BOD@ZIF-90 showed excellent fluorescence response to protamine with a low detection limit of 0.07 μg/mL and the detection was not disturbed by other possible competing substances. Compared with previous methods, BZA-BOD designed by this method is simpler to obtain, and also can achieve sensitive and accurate determination of protamine. Subsequently, the nanocomposite BZA-BOD@ZIF-90 was successfully applied to detect protamine spiked in human serum. In addition, due to the strong binding effect of heparin on protamine, when heparin was added to the complex, the fluorescence intensity of the BZA-BOD@ZIF-90 weakened, thus, it can also be utilized for heparin detection. The medical application of protamine and heparin suggests that this fluorescent molecular device has prospects for certain clinical applications.

1. Introduction

Protamine as an alkaline protein can interact with heparin and is clinically used as heparin neutralizer [1–3] to treat hemorrhage caused by excessive heparin injection [4–6]. Additionally, protamine shows strong bacteriostatic ability and high thermal stability in neutral and alkaline media, so it can also be used as a preservative. Heparin, a natural anticoagulant [7], is a class of highly acidic and negatively charged polysaccharides and mainly used for the treatment of thromboembolic diseases [7–11], myocardial infarction, cardiovascular surgery, cardiac catheterization, cardiopulmonary bypass, hemodialysis in clinic. However, heparin overdose can result in hemorrhage and thrombocytopenia, which are life-threatening. Considering the important physiological and medical functions of protamine and heparin [12–16], developing an effective method to detect these two molecules is of great significance.

In the current clinical trials, the detection of heparin and protamine is based on different strategies, including plasma coagulation, chemical colorimetry [17–19], fluorescence [20,21] and electrophoresis [22]. However, these detection methods are time-consuming, are subject to interference, and require expensive instruments. In addition, many reported methods are based on complex nanomaterials [23–25]. Among these, fluorescence detection is more and more widely used due to its advantages of high sensitivity, good selectivity, low detection limit and real-time detection [4,20,26–28]. However, there still remain the challenging in organic small molecule probes including their high detection limit, poor biocompatibility and solubility.

Metal-organic frameworks (MOFs) have been extensively applied to various fields such as chemical catalysis, biosensor and drug delivery due to their excellent properties including large specific surface area, adjustable topology, excellent photoelectric properties, and high stability [29–34]. An important subclass of MOFs, zeolitic imidazolate frameworks (ZIFs), are widely used for their good biocompatibility, chemical and the high aqueous stability [35–37]. We have observed that some probes are less sensitive when encapsulated within hydrophobic ZIFs like ZIF-8. Additionally, ZIF-8 tends to decompose under particular environment [38]. However, ZIF-90 has a unique aldehyde group structure and is more hydrophilic than other ZIFs. In this case, we encapsulate a probe in the MOFs for the purpose of improving tolerability, stability and biocompatibility of probe, contributing to the improvement of detection performance [39,40].

Herein, we reported a BODIPY-based fluorescent probe encapsulated

* Corresponding authors.
E-mail addresses: shenbx@njnu.edu.cn (B. Shen), zhangxing@njnu.edu.cn (X. Zhang).

https://doi.org/10.1016/j.snb.2021.130006
Received 28 February 2021; Received in revised form 11 April 2021; Accepted 14 April 2021
Available online 19 April 2021

by zeolitic imidazolate framework-90 (ZIF-90). We used BZA-BOD@ZIF-90 for the selective detection of protamine, as shown in Scheme 1. Because traditional probe fluorescence quenching characteristics have certain limitations, our study is based on the AIE mechanism. The mechanism by which they function is that when molecules are in the state of aggregation, intramolecular rotation will be limited, which blocks the non-radiation channel, opens the radiation channel, and increases the molecular fluorescence intensity [8,10,41,42]. In this study, we show that the MOFs probe BZA-BOD@ZIF-90 exhibited good fluorescence response to protamine. Moreover, when heparin was added to the BZA-BOD@ZIF-90/protamine mixture, due to the strong binding effect of heparin and protamine [7,9,43,44], BZA-BOD@ZIF-90 and protamine are separated, so that weaker fluorescence results. Based on this process, BZA-BOD@ZIF-90 can also be used to detect heparin. Additionally, the detection limit of BZA-BOD@ZIF-90 for protamine is as low as 0.07 μg/mL and was successfully applied to detect spiked protamine in human serum. The designing strategy used in this work provides a new approach to develop low-cost tool for detecting protamine.

2. Experimental

2.1. Materials

All the anhydrous organic solvents used in the experiment were purchased from Aladdin (ShangHai, China). The protamine sulfate from salmon and heparin sodium from pig intestine were purchased from BBI Life Sciences Corporation (ShangHai, China) and they were all kept in a 4 °C environment. All inorganic salts used for selective testing of protamine including NH_4HCO_3, $ZnCl_2$, KCl, $CuSO_4$, $FeCl_3$, NaCl, $CaCl_2$, $MgCl_2$ were purchased from the Aladdin (ShangHai, China). Additionally, all organic reagent used in synthetic reactions are purchased from Aladdin (ShangHai, China).

The ultraviolet spectrophotometer and fluorescence spectrophotometer used in this experiment are ultraviolet spectrophotometer (UV 6100A) and fluorospectro photometer (F97Pro19059) respectively. In addition, the fluorescence intensity in this experiment was recorded by the microplate reader (Synergy H1).

2.2. Synthesis of probe BZA-BOD 4-(5,5-difluoro-1,3,7,9-tetramethyl-5H-4,5-dipyrrolo[1,2-c:2′,1′-f][1,3,2]diazaborinin-10-yl)benzoic acid

The 4-carboxybenzaldehyde (1.00 g, 6.7 mmol) was dissolved in 100 mL of DCM in a 500 mL flask. After which 2,4-Dimethylpyrrole (1.39 g, 14.7 mmol) and 3–5 drops trifluoroacetic acid to the mixture were added, noticeable color changes can be observed during this process. The reaction was stirred at room temperature for 12 h. Subsequently, added the oxidant tetra-chloro-benzoquinone (1.64 g, 6.7 mmol) to the mixture for 5 h. Then, 10 mL of triethylamine was added under constant pressure, and 10 mL of boron trifluoride ether complex was added over 30 min in the same environment and stirred at room temperature overnight. Finally, the crude product was purified by silica gel column chromatography (petroleum ether: ethyl acetate = 1: 9) resulting in a pink solid with a green fluorescence (0.12 g, yield: 20.42 %). The characterizations of BZA-BOD were shown in supporting information (Fig. S6-S8). ^{1}H NMR (400 MHz, DMSO) δ 8.12 (dd, J = 8.7, 2.1 Hz, 2 H), 7.58−7.53 (m, 2 H), 6.22 (s, 2 H), 3.37 (s, 13 H), 2.52 (dt, J = 3.6, 1.7 Hz, 3 H), 2.48 (s, 6 H), 1.35 (s, 5 H), 1.25 (s, 2 H), 1.09 (s, 1 H), 1.07 (s, 2 H), 1.06 (s, 1 H). ^{13}C NMR (101 MHz, DMSO) δ 167.33, 155.79, 143.15, 141.30, 138.94, 132.02, 130.79, 130.66, 128.93, 122.11, 56.54, 40.68, 40.47, 40.26, 40.05, 39.84, 39.63, 39.42, 19.06, 14.75, 14.56. LC–MS (m/z): calcd for $C_{20}H_{19}BF_2N_2O_2$, 367.1; observed, 367.3.

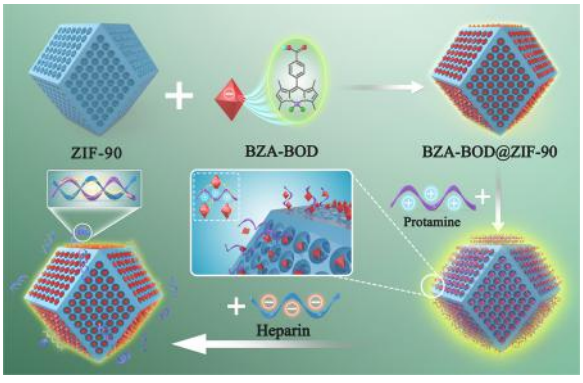

Scheme 1. Schematic diagram of BZA-BOD@ZIF-90 and response to protamine as well as heparin.

2.3. Synthesis of ZIF-90

Imidazole-2-carboxaldehyde (0.24 g, 2.50 mmol) and zinc nitrate (0.12 g, 0.42 mmol) were dissolved in 4 mL H_2O, respectively. Imidazole-2-carboxaldehyde solution was added to the zinc nitrate solution, stired at room temperature overnight, the reaction solution was centrifuged at 8000 rpm for 6 min, and after centrifugation, it was washed with ethanol for 3 times until the supernatant was colorless. Finally, pure ZIF-90 was obtained by vacuum drying.

2.4. Synthesis of BZA-BOD@ZIF-90

First, 4 mL H_2O was added to imidazole-2-carboxaldehyde (0.24 g, 2.50 mmol) and zinc nitrate (0.12 g, 0.42 mmol), respectively. BZA-BOD (0.8 mg) was added to imidazole-2-carboxaldehyde solution in a 250 mL round bottom flask, and then the zinc nitrate solution was added, at room temperature and stirred overnight. Finally, the reaction system was centrifuged at 8000 rpm for 6 min and cleaned with ethanol for 3 times until the supernatant was colorless. After vacuum drying, a powdery white solid powder was obtained.

2.5. Characterization

The spectra of X-Ray photoelectron spectroscopy (XPS) were acquired on a Thermo Scientific ESCALAB™XI with Al κα radiation.

The powder X-ray diffraction (XRD) was obtained using a Rigaku SmartLab at 9 KeV. The X-ray source was generated using Cu κα radiation (λ = 1.5405 Å) with a scanning speed of 10° min^{-1} and the 2θ range between 5° and 35°.

Thermogravimetric analyses (TGA) measurements were carried out on a Pyris 1. TGA with a heating rate of 10 °C min^{-1} under air atmosphere and the temperature range was from 25 to 800 °C.

Fourier transform infrared (FTIR) spectra of the samples were recorded at room temperature on a Vertex 70. Each sample was scanned 25 times at 4 cm^{-1} resolution over the 4000−400 cm^{-1} range.

Scanning electron microscope (SEM) images were collected using Apreo 2S. Prior to analysis, the sample was sprayed with gold and the minimum standard size is 500 nm.

2.6. Fluorescence experiment

2.6.1. Titration

Prior to the titration experiments, the concentration of the materialized probe BZA-BOD@ZIF-90 to be added was determined by the absorbance ratio of the materialized probe and free probe. In the titration experiment, different concentrations of protamine (0 to 0.8 μg mL^{-1}) were incubated with BZA-BOD@ZIF-90 (168 μM) in PBS (10 mM, pH = 7.4) and CH_3CN mixture solution (V_{PBS} : V_{CH3CN} = 1 : 1). Finally, fluorescence intensity of each sample was measured after incubation at 37 °C for 35 min. The results were used to determine the optimal protamine concentration for other response tests.

2.6.2. Selectivity

To detect the selectivity of BZA-BOD@ZIF-90 in the presence of protamine, BOD@ZIF-90 (168 μM) was incubated with various interfering species (0.4 μg mL^{-1}) including NH_4HCO_4, $ZnCl_2$, $CaCl_2$, K_2CO_3, $CuSO_4$, NaCl, KCl, $MgCl_2$ and $FeCl_3$. The detection system was PBS buffer/acetonitrile mixture solution (V_{PBS} : V_{CH3CN} = 1 : 1), and then these mixtures were incubated at 37 °C for 35 min. The selectivity of the protamine was obtained by comparing the fluorescence intensity with that of other interference species.

2.6.3. pH stability

BOD@ZIF-90 (168 μM) and protamine (0.4 μg mL^{-1}) were incubated in different pH environment (ranges from 3 to 10). The detection system was PBS buffer/ acetonitrile mixture solution(V_{PBS} : V_{CH3CN} = 1 : 1). Fluorescence intensity was measured after incubation at 37 °C for 35 min.

3. Results and discussion

3.1. Rational design of MOFs composites BZA-BOD@ZIF-90

In this study, BODIPY was used as fluorescent scaffold due to its excellent photophysical properties including good photochemical stability, easy modification of molecular structure, good tolerance to solvent polarity and different pH environment. A negatively charged carboxyl was introduced into the BODIPY benzene ring to allow it interact with positively charged protamine. However, the small molecule organic fluorescent probe had the defects of poor water solubility and biological compatibility. Recently, it has been demonstrated that hydrophilic ZIF-90 materials have better biocompatibility [29]. On this basis, we used the zeolitic imidazolate framework-90 (ZIF-90) as a shell to prepare BZA-BOD@ZIF-90, in which probe BZA-BOD was encapsulated in ZIF-90 (Scheme 2). Analogous strategies have also been successfully employed to encapsulate and stabilize enzymes to improve their catalytic properties [45]. The experimental results did show that encapsulating the probe in ZIF-90 can effectively improve the detection performance of probe BZA-BOD. Compared with other reported protamine probes, BZA-BOD@ZIF-90 exhibited good sensitivity, high selectivity and excellent biocompatibility.

3.2. Characterization of BZA-BOD@ZIF-90

To confirm that BZA-BOD@ZIF-90 was successfully synthesized, the free ZIF-90 and BZA-BOD@ZIF-90 were investigated using various analytical techniques, including X-Ray photoelectron spectroscopy (XPS), powder X-ray diffraction (XRD), thermogravimetric analysis (TGA) and Fourier transform infrared (FTIR) analysis. As shown in Fig. 1a and b, two signals at 284.80 eV and 398.78 eV were observed in the C1s and N1s regions, consistent with ligand C1s and N1s signals. Additionally, two distinct signal peaks of Zn can be clearly observed, at 1044.70 eV (Zn 2p1/2) and 1021.63 eV (Zn 2p3/2) respectively, which is compatible with Zn^{2+} of the ZIF-90 structure as seen in crystals of this MOF (Fig. 1c). XRD patterns of BZA-BOD@ZIF-90 indicate a reduced crystallinity of probe-MOF composites, compared to the pure ZIF-90 obtained in solution synthesis. The reason for this may be the interaction of the carboxyl group on the benzene ring and zinc lead to the XRD phase was not pure (Fig. 1d).

The thermogravimetric analysis profile was showed in Fig. 1e, three plateaus appeared, which implied two evident mass loss behaviors. The original weight loss in temperature range 140 °C–200 °C that might be attributed to the removal of unreacted species (imidazole-2-carboxaldehyde) and water molecules inside the pores or elsewhere within the framework. The second weight loss from 200 °C to 660 °C could cause from the framework deformation. However, compared with ZIF-90, BZA-BOD@ZIF-90 showed a more obvious weight loss in temperature range 140 °C–660 °C, which could be due to the loss of probe. We can see that after heated to 660 °C, 5 % weight of BZA-BOD@ZIF-90 and 15 % weight of ZIF-90 remained. Generally speaking, the loss of weight suggested that the BZA-BOD was verified to encapsulate in ZIF-90 successfully. As for FTIR results that shown in Fig. 1f, the peaks at 1450 cm^{-1}, 1360 cm^{-1}, 1170 cm^{-1}, 951 cm^{-1}, and 789 cm^{-1} were reasonably attributed to characteristic absorption of imidazole moieties of ZIF-90. Moreover, the peaks at 2858 cm^{-1} and 1670 cm^{-1} could be formed by the C—H and C═O stretching vibration of aldehyde groups. In addition, due to the C—O stretching vibration on carboxyl group and the substituent groups bending vibration on benzene ring of the BZA-BOD@ZIF-90 is respectively near the peak of 1300 cm^{-1} and 840 cm^{-1}, the peaks are denser in low wavenumber [46]. Besides above characterization analysis, we also explored the morphology of BZA-BOD@ZIF-90 through SEM in Fig. S5. These results indicate that BZA-BOD@ZIF-90 was successfully synthesized.

3.3. Photophysical properties and fluorescence response of BZA-BOD@ZIF-90 to protamine

We first investigated the absorption and emission wavelengths of BZA-BOD, it is observed from Fig. 2a that the maximum absorbance wavelength of BZA-BOD located at 498 nm, and the maximum emission wavelength was observed at 509 nm. The fluorescence quantum yield of BZA-BOD was calculated as 20.42 %. Table 1 is the basic photophysical properties of BZA-BOD. As described in Fig. 2b, the intensive fluorescence of BZA-BOD@ZIF-90/protamine can be observed by the fluorescence spectra after the protamine was added. This enhanced fluorescence phenomenon caused by the addition of protamine may be caused by the aggregation of BODIPY molecule after the addition of protamine, which opens the radiation channel and leads to the enhancement of fluorescence. After determining that BZA-BOD@ZIF-90 does have a response to protamine, the difference of the relative fluorescence intensity before and after the addition of protamine was measured in Fig. 2c. The relationship between fluorescence intensity and the incubation time of BZA-BOD@ZIF-90/PRTM is shown in Fig. S1. It is easy to conclude that the fluorescence intensity reaches the maximum at 25 min after the addition of protamine and the detection can be completed within 35 min. The fluorescence intensity of BZA-BOD@ZIF-90 in the presence of protamine, as well as other interfering cation, was measured to verify the selectivity of the BZA-BOD@ZIF-90 to protamine. As shown in Fig. 2d, almost no fluorescence changes of BZA-BOD@ZIF-90 could be observed when incubated with other species

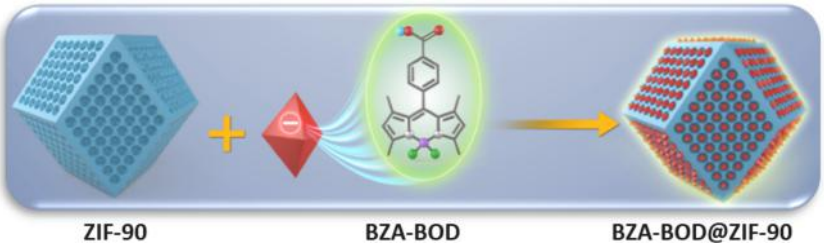

Scheme 2. The synthesis of MOFs probe BZA-BOD@ZIF-90.

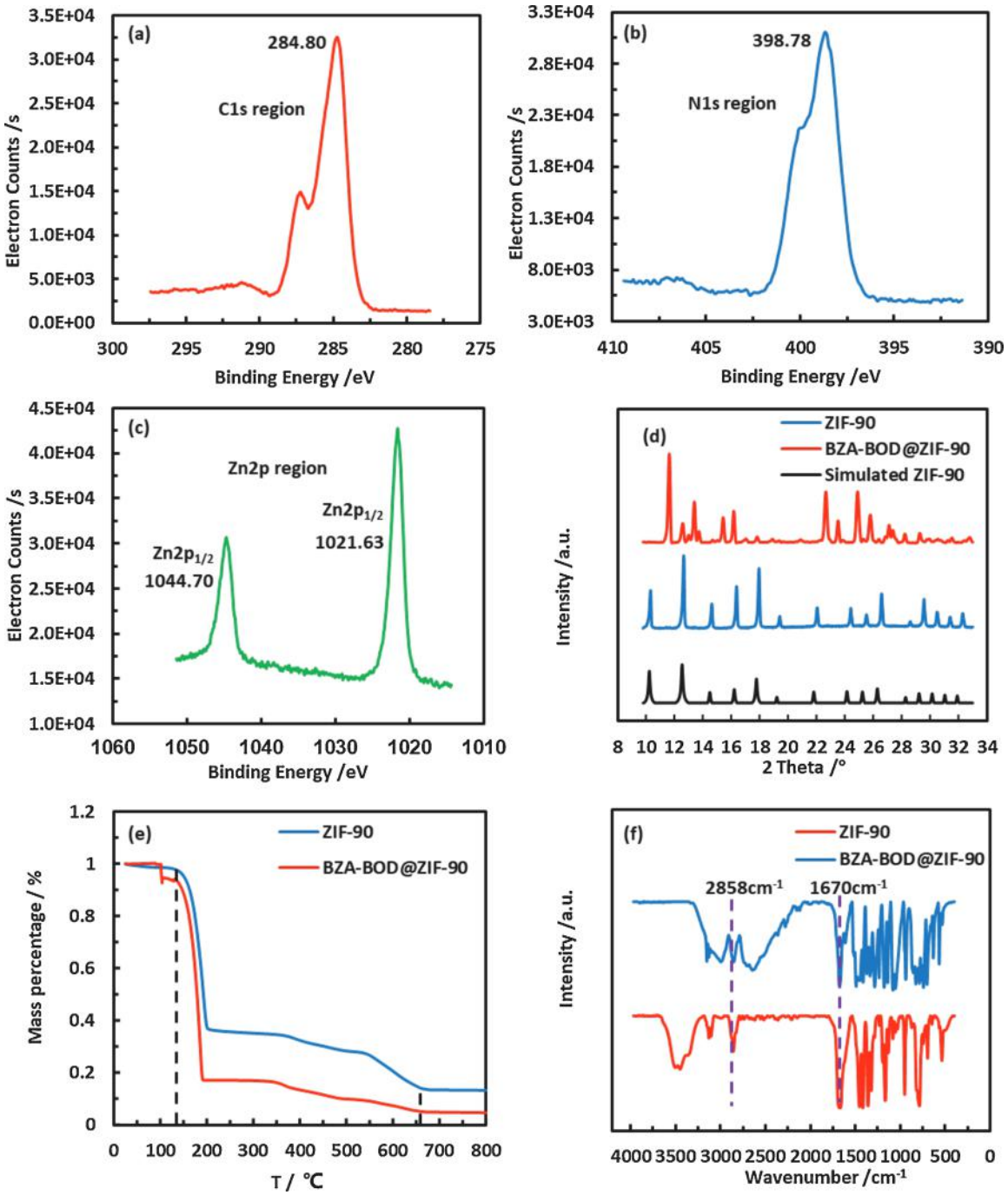

Fig. 1. Characterization of BZA-BOD@ZIF-90. (a) XPS spectra of the BZA-BOD@ZIF-90 in C1s region, (b) N1s region and (c) Zn 2p region; (d) XRD patterns of simulated ZIF-90, ZIF-90 and BZA-BOD@ZIF-90; (e) TGA curve of the ZIF-90 and BZA-BOD@ZIF-90; (f) FTIR spectra of ZIF-90 and BZA-BOD@ZIF-90.

including NH_4^+, Zn^{2+}, Ca^{2+}, K^+, Cu^{2+}, Na^+, Mg^{2+} and Fe^{3+}. However, a significant fluorescence intensity enhancement was observed after the addition of protamine, which indicate that BZA-BOD@ZIF-90 was highly selective to protamine.

3.4. BZA-BOD@ZIF-90 served as viscometer for monitoring microenvironmental changes

We next investigated the viscosity sensitivity properties of BZA-BOD@ZIF-90. It was interesting to find out that BZA-BOD@ZIF-90 have aggregation-induced emission (AIE) properties. We observed that the relative fluorescence intensity of BZA-BOD@ZIF-90 showed an excellent liner relationship with an increase of viscosity (Fig. 3a). The fluorescence intensity of BZA-BOD@ZIF-90 gradually enhanced with the increase of the glycerol proportion in glycerol/water mixtures (Fig. 3b and Fig. S2). The reason for this may be that when molecules were in the state of aggregation, the rotation of the single bond connected with a benzene ring will be restricted, which blocks the non-radiation channel, opens the radiation channel, and increased the molecular fluorescence intensity.

3.5. Quantitative determination of protamine and heparin

For the purpose of determining the sensitivity of BZA-BOD@ZIF-90 to protamine detection, we carried out protamine titration experiments. When the protamine concentration increased from 0.15 μg mL^{-1}

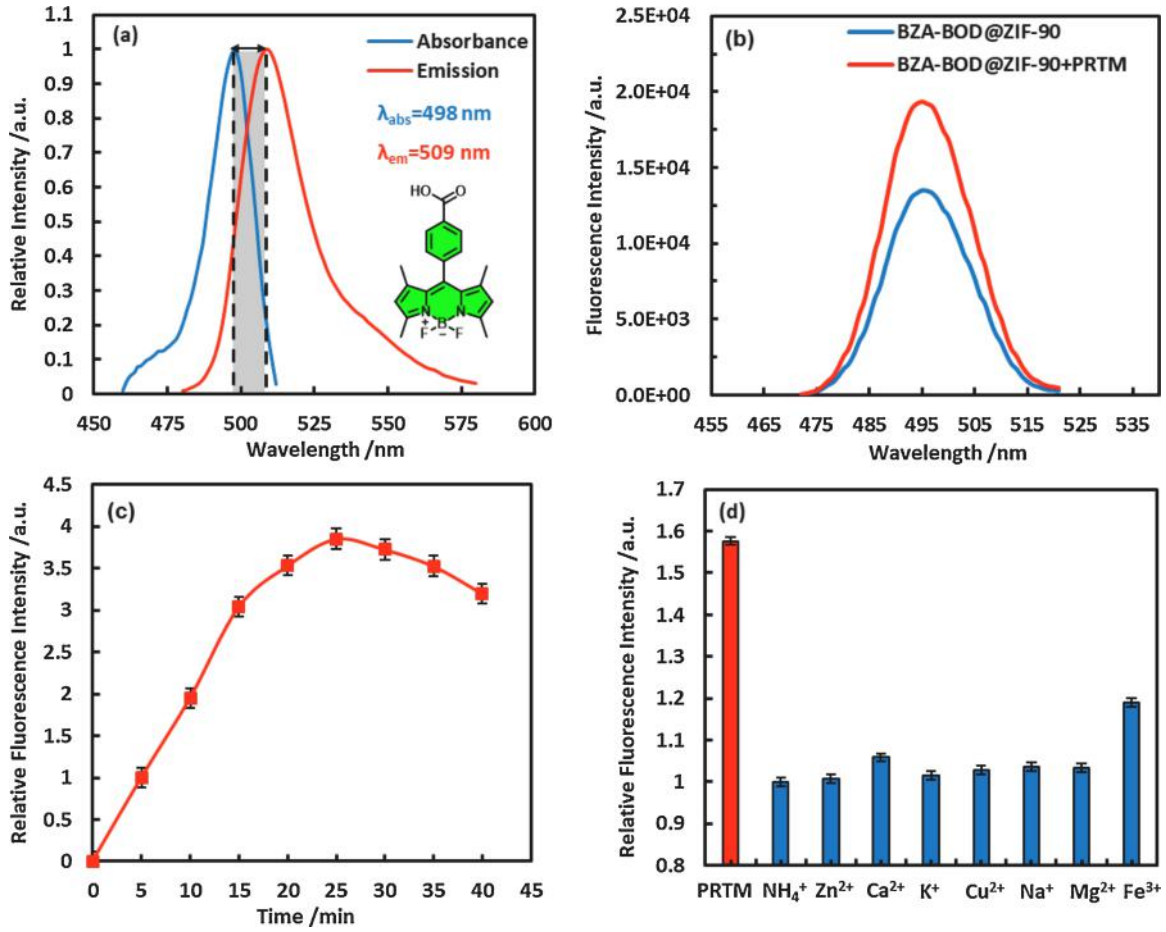

Fig. 2. (a) Relative absorbance and emission spectra of BZA-BOD (10 μM) in PBS buffer (containing less than 1% DMSO) at 25 °C; (b) Fluorescence responses of the free BZA-BOD@ZIF-90 (168 μM) and BZA-BOD@ZIF-90/protamine mixture; (c) Relative fluorescence intensity of BZA-BOD@ZIF-90 (168 μM) in the presence of protamine (0.4 μg mL^{-1}) as a function of increasing incubation time; (d) Relative fluorescence intensity of BZA-BOD@ZIF-90 (168 μM) incubated with various cations, and the minimum fluorescence intensity at 509 nm was normalized to 1 ($C_{protamine}$ = 0.4 μg mL^{-1}), $C_{cations}$ = 20 μM, PBS buffer 10 mM pH 7.4, V_{PBS}: V_{CH3CN} = 1:1, incubated at 37 °C for 35 min).

Table 1
Basic Photophysical data of BZA-BOD.

Compound	λ_{em}[a] (nm)	λ_{abs}[b] (nm)	φ[c]	ε[d] (M^{-1}c m^{-1})	B[e] (M^{-1} cm^{-1})	Δλ[f] (nm)
BZA-BOD	509	498	0.20	1.05×10^4	2.2×10^3	11

[a] The maximum emission wavelength.
[b] The maximum absorption wavelength.
[c] The fluorescence quantum yield (measured in 50 % PBS-50 % CH_3CN).
[d] The molar extinction coefficient.
[e] Brightness (B) was calculated using B = φ*ε.
[f] Stokes shift t was calculated as Δλ = λ_{em} - λ_{abs}.

to 0.8 μg mL^{-1}, the fluorescence intensity of BZA-BOD@ZIF-90 increased gradually after the addition of protamine. A good linear relationship of fluorescence intensity changes can be observed in the range of 0.25 to 0.4 μg mL^{-1} (Fig. 4a). According to the formula 3σ/k, where σ is the standard deviation of the blank probe (the number of independent experiment is n = 10), k is the slope of titration experiment. The detection limit of BZA-BOD@ZIF-8 to protamine was calculated as low as 0.07 μg/mL, which was much lower than the reported method for the determination of protamine (Table S1).

We known that heparin is a negatively charged glycosaminoglycan with a high binding affinity for protamine. After determining the responsiveness and sensitivity of the probe to protamine, we further investigated whether adding heparin would affect the response of BZA-BOD@ZIF-90 to protamine. Since the addition of protamine would enhance the fluorescence of the BZA-BOD@ZIF-90, we speculated that the addition of heparin would compete with the protamine and caused the complex formed by protamine and BZA-BOD@ZIF-90 to disintegrate, thus a fluorescence decrease would be observed. As speculated, we recorded the fluorescence intensity of BZA-BOD@ZIF-90/protamine complex after incubating with different concentrations of heparin. The results showed that the fluorescence intensity exhibited a downward trend with the increase of heparin concentration and had a good linear relationship in the range of 2.0 to 2.5 μg mL^{-1} (Fig. 4b). These results indicated that BZA-BOD@ZIF-90 can be applied to quantitative detection of protamine and heparin. The titration experiments of BZA-BOD was also explored and shown in supporting information (Fig. S3).

3.6. pH stability

The fluorescence intensity changes of BZA-BOD@ZIF-90 with protamine was measured in a wide range of pH values from 3 to 10 to investigate the applicability of BZA-BOD@ZIF-90 for detecting protamine in different environments. The relative fluorescence intensity of BZA-BOD@ZIF-90/protamine in different pH solutions with the fluorescence intensity at pH 7 normalized to 1 is shown in Fig. 5. It is clear that under different pH conditions the fluorescence intensity of BZA-BOD@ZIF-90/protamine remained stable with almost no fluctuation. This demonstrates that the BZA-BOD@ZIF-90 shows good stability in the detection of protamine in physiological environments.

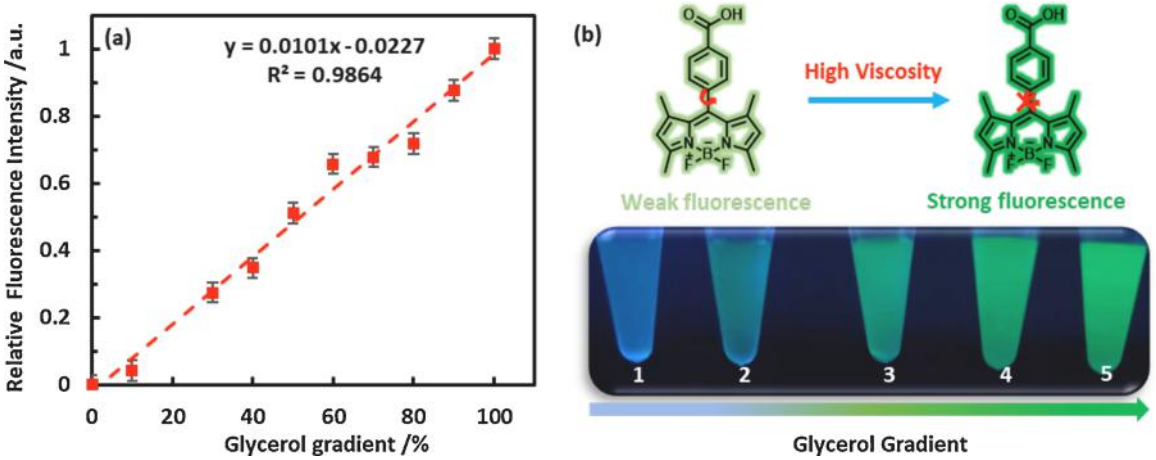

Fig. 3. (a) Relative fluorescence intensity changes of BZA-BOD@ZIF-90 in various glycerol/water mixture solutions with different glycerol concentrations; (b) Fluorescence images of BZA-BOD@ZIF-90 in various mixture solutions with different glycerol concentrations (1: 10 % glycerol, 2: 30 % glycerol, 3: 50 % glycerol, 4: 70 % glycerol, 5: 90 % glycerol).

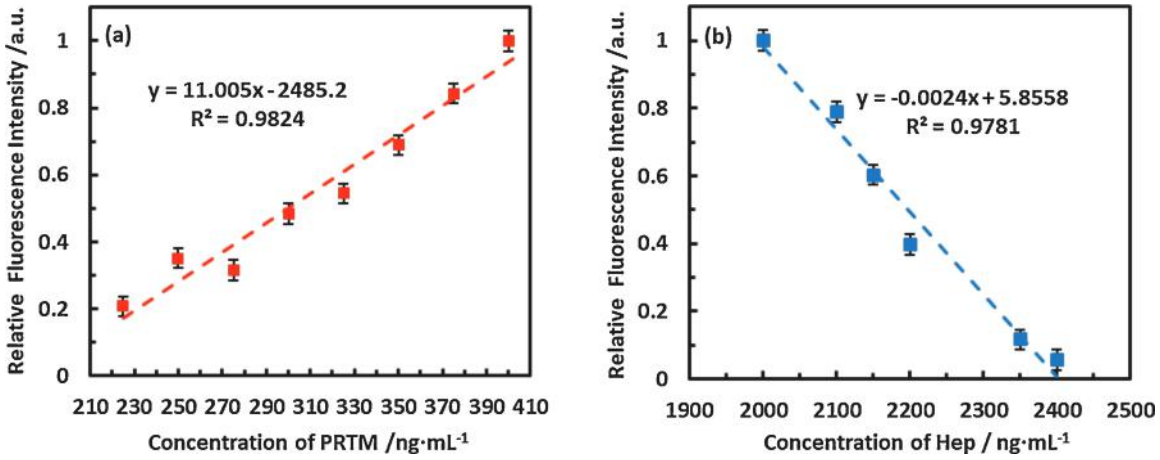

Fig. 4. (a) Fluorescence intensity changes of BZA-BOD@ZIF-90 (168 μM) incubated with different concentrations of protamine; (b) Fluorescence intensity changes of BZA-BOD@ZIF-90 (168 μM) incubated with different concentrations of heparin.

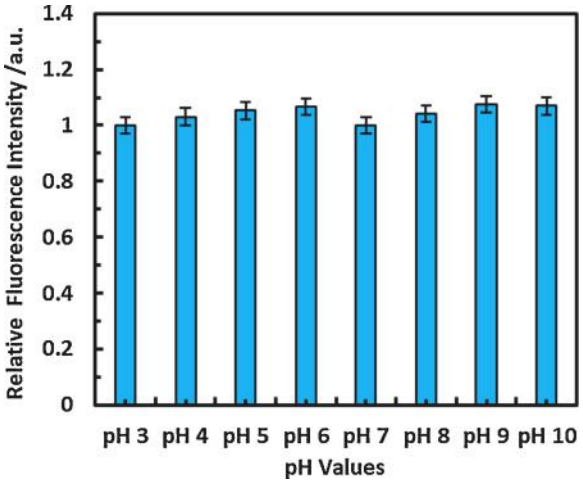

Fig. 5. Relative fluorescence intensity changes of BZA-BOD@ZIF-90 (168 μM) in PBS buffer with different pH in the presence of protamine (0.4 μg/mL).

3.7. Real application in serum samples

Finally, to assess the practical application of BZA-BOD@ZIF-90 for protamine detection in complex matrixes, we applied the BZA-BOD@ZIF-90 to detect spiked protamine in three human serum samples. We used the standard additive recovery method to detect protamine and the results are summarized in Table 2. For targets at concentrations located in the dynamic detection range of BZA-BOD@ZIF-90, the recovery of the spiked protamine in real samples displayed an excellent performance, and the relative standard deviations (RSD) were lower than 4%. The results indicate that BZA-BOD@ZIF-90 is a promising detection platform for monitoring protamine in real biological samples with good reproducibility, high accuracy and sensitivity, as well as good biocompatibility.

Table 2
Recovery of spiked protamine in human serum samples.

Added (ng mL^{-1})	Found (ng mL^{-1})	Recovery (%)	R.S.D[a] (%, n = 3)
150	153.9	102.6	2.96
250	252.5	101	2.67
350	358.5	102.4	3.57

[a] R.S.D: Relative Standard Deviations.

4. Conclusion

We have successfully constructed a sensitive probe BZA-BOD@ZIF-90 for detecting protamine by taking advantage of AIE effect, the low detection limit for protamine with BZA-BOD@ZIF-90 can reach 0.07 μg/mL. The introduction of hydrophilic ZIF-90 materials provides a probe BZA-BOD@ZIF-90 with good biocompatibility, high selectivity, and excellent pH stability. Also, BZA-BOD@ZIF-90 was applied for the quantitative detection of heparin. The synthesis of BZA-BOD@ZIF-90 suggests the possibility for the detection in real samples. We expect that the strategy used in this work may offer a new approach to develop low-cost tool for other biological and environmental applications.

CRediT authorship contribution statement

Lihua Liu: Writing - original draft, Data curation. **Jianan Dai:** Data curation. **Yuan Ji:** Data curation. **Baoxing Shen:** Writing - review & editing, Supervision. **Xing Zhang:** Writing - review & editing, Supervision. **Robert J. Linhardt:** Writing - review & editing.

Declaration of Competing Interest

The authors report no declarations of interest.

Acknowledgements

This work was financially supported by the “Youth Program of National Natural Science Foundation” of China (Grant No. 22007048), Natural Science Foundation of the Jiangsu Higher Education Institutions of China (20KJB150046), Science and Technology Innovation Project for Overseas Students of Nanjing in 2020 (184080H201148), Jiangsu innovation and entrepreneurship doctoral program to Baoxing Shen, Natural Science Foundation of Jiangsu Province (BK20200728), and Jiangsu Specially-Appointed Professor Project to Xing Zhang.

Appendix A. Supplementary data

Supplementary material related to this article can be found, in the online version, at doi:https://doi.org/10.1016/j.snb.2021.130006.

References

[1] S.P. Pandey, P. Jha, P.K. Singh, Aggregation induced emission of an anionic tetraphenylethene derivative for efficient protamine sensing, J. Mol. Liq. 315 (2020).
[2] X. Wang, Q. Jiang, Y. Man, S. Feng, Y.-I. Lee, H.-G. Liu, A novel amphiphilic pH-responsive AIEgen for highly sensitive detection of protamine and heparin, Sens. Actuators B Chem. 261 (2018) 233–240.
[3] A.A. Ensafi, N. Kazemifard, B. Rezaei, A simple and rapid label-free fluorimetric biosensor for protamine detection based on glutathione-capped CdTe quantum dots aggregation, Biosens. Bioelectron. 71 (2015) 243–248.
[4] H. Cheng, Y. Zhao, H. Xu, Y. Hu, L. Zhang, G. Song, et al., Rapid and visual detection of protamine based on ionic self-assembly of a water soluble perylene diimide derivative, Dye. Pigment. 180 (2020).
[5] Y.Q. Lv, S. Ji, X. Chen, D. Xu, X.T. Luo, M.M. Cheng, et al., Effects of crocin on frozen-thawed sperm apoptosis, protamine expression and membrane lipid oxidation in Yanbian yellow cattle, Reprod. Domest. Anim. 55 (2020) 1011–1020.
[6] Q. Huang, J. Zhang, W. Li, Y. Fu, A heparin-modified palladium nanozyme for photometric determination of protamine, Mikrochim. Acta 187 (2020) 226.
[7] J. Zheng, T. Ye, J. Chen, L. Xu, X. Ji, C. Yang, et al., Highly sensitive fluorescence detection of heparin based on aggregation-induced emission of a tetraphenylethene derivative, Biosens. Bioelectron. 90 (2017) 245–250.
[8] Y. Gao, K. Wei, J. Li, Y. Li, J. Hu, A facile four-armed AIE fluorescent sensor for heparin and protamine, Sens. Actuators B Chem. 277 (2018) 408–414.
[9] Q. Huang, H. Zhao, M. Shui, D.-S. Guo, R. Wang, Heparin reversal by an oligoethylene glycol functionalized guanidinocalixarene, Chem. Sci. 11 (2020) 9623–9629.
[10] R. Jiang, S. Zhao, L. Chen, M. Zhao, W. Qi, W. Fu, et al., Fluorescence detection of protamine, heparin and heparinase II based on a novel AIE molecule with four carboxyl, Int. J. Biol. Macromol. 156 (2020) 1153–1159.
[11] Y. Yu, K. Bruzdoski, V. Kostousov, L. Hensch, S.K. Hui, F. Siddiqui, et al., Structural characterization of a clinically described heparin-like substance in plasma causing bleeding, Carbohydr. Polym. 244 (2020), 116443.
[12] A. Ranger, M. Gaspar, A. Elkhatteb, T. Jackson, S. Fox, T.C. Aw, et al., The heparin-von Willebrand factor interaction and conventional tests of haemostasis - the challenges in predicting bleeding in cardiopulmonary bypass, Br. J. Haematol. (2020).
[13] L.-C. Chang, H.-F. Lee, M.-J. Chung, V.C. Yang, PEG-modified protamine with improved Pharmacological/Pharmaceutical properties as a potential protamine substitute: synthesis and in vitro evaluation, Bioconjug. Chem. 16 (2005) 147–155.
[14] J.V. Gonzalez-Aramundiz, M. Peleteiro, A. Gonzalez-Fernandez, M.J. Alonso, N. S. Csaba, Protamine nanocapsules for the development of thermostable adjuvanted nanovaccines, Mol. Pharm. 15 (2018) 5653–5664.
[15] Y.Y. Liu, X.F. Chen, J.W. Hu, Z.W. Chen, L.J. Zhang, M.J. Cao, et al., Purification and characterization of protamine, the allergen from the milt of large yellow croaker (Pseudosciaena crocea), and its components, J. Agric. Food Chem. 64 (2016) 1999–2011.
[16] Q. Yang, J. Li, X. Wang, H. Peng, H. Xiong, L. Chen, Strategies of molecular imprinting-based fluorescence sensors for chemical and biological analysis, Biosens. Bioelectron. 112 (2018) 54–71.
[17] R. Badugu, J.R. Lakowicz, C.D. Geddes, Enhanced fluorescence cyanide detection at physiologically lethal levels: reduced ICT-based signal transduction, J. Am. Chem. Soc. 127 (2005) 3635–3641.
[18] G.A. Crespo, M.G. Afshar, D. Dorokhin, E. Bakker, Thin layer coulometry based on ion-exchanger membranes for heparin detection in undiluted human blood, Anal. Chem. 86 (2014) 1357–1360.
[19] Q. Chen, X. Li, R. Wang, F. Zeng, J. Zhai, X. Xie, Rapid equilibrated colorimetric detection of protamine and heparin: recognition at the nanoscale liquid-Liquid interface, Anal. Chem. 91 (2019) 10390–10394.
[20] S.Y. Hung, W.L. Tseng, A polyadenosine-coralyne complex as a novel fluorescent probe for the sensitive and selective detection of heparin in plasma, Biosens. Bioelectron. 57 (2014) 186–191.
[21] H. Yukawa, M. Watanabe, N. Kaji, Y. Okamoto, M. Tokeshi, Y. Miyamoto, et al., Monitoring transplanted adipose tissue-derived stem cells combined with heparin in the liver by fluorescence imaging using quantum dots, Biomaterials 33 (2012) 2177–2186.
[22] H. Qi, L. Zhang, L. Yang, P. Yu, L. Mao, Anion-exchange-based amperometric assay for heparin using polyimidazolium as synthetic receptor, Anal. Chem. 85 (2013) 3439–3445.
[23] Y. Ding, X. Li, T. Li, W. Zhu, Y. Xie, Alpha-Monoacylated and alpha,alpha'- and alpha,beta'-diacylated dipyrrins as highly sensitive fluorescence "turn-on" Zn2+ probes, J. Org. Chem. 78 (2013) 5328–5338.
[24] J. Liu, G. Liu, W. Liu, Y. Wang, Turn-on fluorescence sensor for the detection of heparin based on rhodamine B-modified polyethyleneimine-graphene oxide complex, Biosens. Bioelectron. 64 (2015) 300–305.
[25] Z. Ding, C. Wang, S. Wang, L. Wu, X. Zhang, Light-harvesting metal-organic framework nanoprobes for ratiometric fluorescence energy transfer-based determination of pH values and temperature, Mikrochim. Acta 186 (2019) 476.
[26] Q. Dai, W. Liu, X. Zhuang, J. Wu, H. Zhang, P. Wang, Ratiometric fluorescence sensor based on a pyrene derivative and quantification detection of heparin in aqueous solution and serum, Anal. Chem. 83 (2011) 6559–6564.
[27] D.H. Kim, Y.J. Park, K.H. Jung, K.H. Lee, Ratiometric detection of nanomolar concentrations of heparin in serum and plasma samples using a fluorescent chemosensor based on peptides, Anal. Chem. 86 (2014) 6580–6586.
[28] L.J. Chen, Y.Y. Ren, N.W. Wu, B. Sun, J.Q. Ma, L. Zhang, et al., Hierarchical self-assembly of discrete organoplatinum(II) metallacycles with polysaccharide via electrostatic interactions and their application for heparin detection, J. Am. Chem. Soc. 137 (2015) 11725–11735.
[29] F.M. Zhang, H. Dong, X. Zhang, X.J. Sun, M. Liu, D.D. Yang, et al., Postsynthetic modification of ZIF-90 for potential targeted codelivery of two anticancer drugs, ACS Appl. Mater. Interfaces 9 (2017) 27332–27337.
[30] D. Hua, Y.K. Ong, Y. Wang, T. Yang, T.-S. Chung, ZIF-90/P84 mixed matrix membranes for pervaporation dehydration of isopropanol, J. Membr. Sci. 453 (2014) 155–167.
[31] J.A. Gee, J. Chung, S. Nair, D.S. Sholl, Adsorption and diffusion of small alcohols in zeolitic imidazolate frameworks ZIF-8 and ZIF-90, J. Phys. Chem. C 117 (2013) 3169–3176.
[32] W. Morris, C.J. Doonan, H. Furukawa, R. Banerjee, O.M. Yaghi, Crystals as molecules: postsynthesis covalent functionalization of zeolitic imidazolate frameworks, J. Am. Chem. Soc. 130 (2008) 12626–12627.
[33] A. Karmakar, N. Kumar, P. Samanta, A.V. Desai, S.K. Ghosh, A post-synthetically modified MOF for selective and sensitive aqueous-phase detection of highly toxic cyanide ions, Chemistry 22 (2016) 864–868.
[34] F. Qu, X. Li, X. Lv, J. You, W. Han, Highly selective metal–organic framework-based sensor for protamine through photoinduced electron transfer, J. Mater. Sci. 54 (2018) 3144–3155.
[35] Y. Pan, Y. Liu, G. Zeng, L. Zhao, Z. Lai, Rapid synthesis of zeolitic imidazolate framework-8 (ZIF-8) nanocrystals in an aqueous system, Chem. Commun. (Camb.) 47 (2011) 2071–2073.
[36] R. Zou, Q. Gong, Z. Shi, J. Zheng, J. Xing, C. Liu, et al., A ZIF-90 nanoplatform loaded with an enzyme-responsive organic small-molecule probe for imaging the hypoxia status of tumor cells, Nanoscale 12 (2020) 14870–14881.
[37] B. Shen, C. Ma, Y. Ji, J. Dai, B. Li, X. Zhang, et al., Detection of carboxylesterase 1 and chlorpyrifos with ZIF-8 metal-organic frameworks using a red emission BODIPY-based probe, ACS Appl. Mater. Interfaces 13 (2021) 8718–8726.
[38] J. Deng, K. Wang, M. Wang, P. Yu, L. Mao, Mitochondria targeted nanoscale zeolitic imidazole Framework-90 for ATP imaging in live cells, J. Am. Chem. Soc. 139 (2017) 5877–5882.

[39] A. Ojida, T. Sakamoto, M.A. Inoue, S.H. Fujishima, G. Lippens, I. Hamachi, Fluorescent BODIPY-based Zn(II) complex as a molecular probe for selective detection of neurofibrillary tangles in the brains of Alzheimer's disease patients, J. Am. Chem. Soc. 131 (2009) 6543–6548.
[40] C. Ma, J. Wu, W. Sun, Y. Hou, G. Zhong, R. Gao, et al., A near infrared BODIPY-based lysosome targeting probe for selectively detection of carboxylesterase 1 in living cells pretreated with pesticides, Sens. Actuators B Chem. 325 (2020).
[41] C. Ma, W. Sun, L. Xu, Y. Qian, J. Dai, G. Zhong, et al., A minireview of viscosity-sensitive fluorescent probes: design and biological applications, J. Mater. Chem. B 8 (2020) 9642–9651.
[42] H. Zhu, Q. Li, B. Shi, F. Ge, Y. Liu, Z. Mao, et al., Dual-emissive platinum(II) metallacage with a sensitive oxygen response for imaging of hypoxia and imaging-guided chemotherapy, Angew. Chem. Int. Ed. Engl. (2020).
[43] H. Lee, B. In, P.K. Mehta, M. Kishore, K.H. Lee, Dual role of a fluorescent peptidyl probe based on self-assembly for the detection of heparin and for the inhibition of the heparin-digestive enzyme reaction, ACS Appl. Mater. Interfaces 10 (2018) 2282–2290.
[44] J.C. Sistla, S. Morla, A.B. Alabbas, R.C. Kalathur, C. Sharon, B.B. Patel, et al., Polymeric fluorescent heparin as one-step FRET substrate of human heparanase, Carbohydr. Polym. 205 (2019) 385–391.
[45] B. Shen, X. Zhang, J. Dai, Y. Ji, H. Huang, Lysosome targeting metal-organic framework probe LysFP@ZIF-8 for highly sensitive quantification of carboxylesterase 1 and organophosphates in living cells, J. Hazard. Mater. (2020), 124342.
[46] T. Taghizadeh, A. Ameri, A. Talebian-Kiakalaieh, S. Mojtabavi, A. Ameri, H. Forootanfar, et al., Lipase@zeolitic imidazolate framework ZIF-90: a highly stable and recyclable biocatalyst for the synthesis of fruity banana flavour, Int. J. Biol. Macromol. 166 (2021) 1301–1311.

Lihua Liu In September 2020, Lihua Liu joined Baoxing Shen's group at the Institute of Biological and Chemical Sciences, School of Food Science and Pharmaceutical Engineering, Nanjing Normal University. She is currently studying for a master's degree. Her recent researches are focus on the detection mechanism and design concept of fluorescent probes.

Jianan Dai obtained her B.E. in July 2019 from Jiangsu Ocean University in China. In September 2019, she joined Baoxing Shen's group at the Institute of Biological and Chemical Sciences, School of Food Science and Pharmaceutical Engineering, Nanjing Normal University. She is currently studying for a master's degree. Her recent researches are focus on the detection mechanism and design concept of fluorescent probes.

Baoxing Shen obtained his PhD degrees in Materials Physics and Chemistry from Southeast University in 2019, China, under the guidance of Professor Ying Qian. After that, he joined Nanjing Normal University (2019), China. He is currently a faculty member of the School of Food Science and Pharmaceutical Engineering at Nanjing Normal University, China. His researches focus on organic fluorescent probe and sensors chemistry. He has authored over 20 articles including *ACS Appl Mater Interfaces, J Hazard Mater, Sensors and Actuators B: Chemical and etc.*

Xing Zhang was born in Hunan (China) in 1987. He received a B.Sc. from Beijing Normal University in 2009 and completed Ph.D. studies at Chinese Academy of Sciences under the supervision of Prof. Yuguo Du in 2014. He joined Prof. Robert J. Linhardt's group at Rensselaer Polytechnic Institute (U.S.) in 2015 and work as a postdoctoral associate focusing on carbohydrate chemistry, a topic that he has continued to work since joining Nanjing Normal University (China) as a full professor in 2019. He has authored over 50 articles including *PNAS*, *Accounts of Chemical Research* and *Chemical Science*.

Robert J. Linhardt received his Ph.D. in chemistry from Johns Hopkins University in 1979 and did his postdoctoral studies at Massachusetts Institute of Technology. He is currently the Anne and John Broadbent, Jr.' 59 Senior Constellation Chair in Biocatalysis and Metabolic Engineering at Rensselaer Polytechnic Institute. His research focuses on glycoscience, and he is an expert on glycosaminoglycans and their synthesis, biology, and analysis. He has received multiple honors, including the National Academy of Inventors (NAI) Fellow, American Chemical Society Horace S. Isbell, Claude S. Hudson, and Melville L. Wolfrom Awards, the AACP Volwiler Research Achievement Award, the Society of Glycobiology Karl Meyer Award, and the Scientific American 10.